Journal of Applied Electrochemistry **29**: 1297–1304, 1999.

Electrodeposition of Zn and In onto vitreous carbon

A.G. MUÑOZ, S.B. SAIDMAN and J.B. BESSONE*
Instituto de Ingeniería Electroquímica y Corrosión (INIEC), Departamento de Química e Ingeniería Química, Universidad Nacional del Sur, Av. Alem 1253-8000-Bahía Blanca, Argentina
*(*author for correspondence, e-mail: jbessone@criba.edu.ar)*

Received 24 December 1998; accepted in revised form 13 April 1999

Key words: electrodeposition, indium, vitreous carbon, zinc

Abstract

The deposition of indium and zinc on vitreous carbon was studied by voltammetric, galvanostatic and single potentiostatic pulse techniques. The morphology and composition of deposits were analysed by SEM/EDX. The codeposition process occurs without the formation of alloys or intermetallic compounds. On the one hand under stagnant conditions or at low electrode rotation speeds, localized alkalization produced by the hydrogen evolution reaction (HER) favours deposition through an indium hydroxide layer, and deposits with the same atomic percentage of In and Zn are attained. On the other hand, under electrode rotation, preferred deposition of Zn takes place. In this case, the reduction of H^+ by the In^+ species, intermediate in the In^{3+} reduction process, diminishes the electrochemical HER on the substrate thus favouring Zn deposition. The higher nucleation rate on metallic deposits previously formed on the vitreous carbon surface is also likely.

1. Introduction

The sufficiently negative active potential and the high current efficiency shown by Al–Zn–In alloy (operating in chloride media) are factors which favour their application in primary batteries or as sacrificial anodes in cathodic protection [1]. The synergistic effect exerted by Zn and In on the aluminium activation process has not yet been explained, especially those effects dealing with the operating potential and current efficiency [2]. Thus, the performance of an aluminium anode is strongly influenced by its microstructure, where the distribution of alloying elements play an important role.

The cathodic polarization of Al in acidic solutions in the presence of In^{3+} and Zn^{2+} was used as a method of generating surface conditions similar to those found in Al–Zn–In alloys [3–5]. In this way similar active properties can be attained. Previous work on the deposition process of both ions onto Al showed that the presence of Zn^{2+} in the solution promoted In deposition without rotation [4]. However, under rotation and at low cathodic overpotentials, Zn^{2+} discharge became the prevalent reaction [6]. Study of the codeposition onto Al is very complex due to the presence of Al oxide and the onset of pitting. The aim of the present work is to analyse the electrodeposition process using an inert substrate, here vitreous carbon (VC). Thus, a better understanding of the influence of the electrolyte and the hydrodynamic conditions on the deposit composition and morphology may be obtained.

2. Experimental details

The experimental set-up was described previously [4]. Vitreous carbon rods embedded in a Teflon holder with an exposed area of 0.070 cm^2 were used as working electrodes. The electrodes were polished with 1000 emery paper, 1 μm and 0.3 μm grit alumina suspensions, then cleaned with triply distilled water and wiped with filter paper. The auxiliary electrode was a large Pt sheet. As references electrodes, a saturated calomel electrode (SCE) and a $Hg/Hg_2SO_4(s)/Na_2SO_4(sat)$ electrode were used in solutions with and without chloride, respectively. All potentials in the text are referred to SCE.

Runs were made in 0.5 M NaCl or 0.5 M Na_2SO_4 solutions containing In^{3+}, Zn^{2+} or both ions in 0.01 M concentration and in a purified nitrogen gas saturated atmosphere at 25 °C. The pH of the solutions was adjusted by addition of HCl or H_2SO_4. The solutions were prepared from analytical grade chemicals with triply distilled water.

The anodic stripping of the deposits was performed under stagnant condition at 0.005 V s^{-1} in 0.5 M Na_2SO_4, pH 3 solution, without the presence of depositing cations.

Current–potential responses were obtained using a linear voltage sweep generator PAR model 175, a potentiostat–galvanostat PAR model 173 and an X–Y HP 4007B recorder. Current–time responses were recorded with Datalab transient recorder model DL902. A dual stage ISI DS 130 SEM and an EDAX 9600 quantitative

energy dispersive analyser were used to examine the morphology and composition of the deposits.

3. Results and discussion

3.1. *Electrodeposition of In and Zn without electrode rotation*

Figure 1 shows the voltammograms of VC recorded in 0.5 M Cl^- solution in the presence of 0.01 M In^{3+} + 0.01 M Zn^{2+} and those obtained in the presence of only one of the cations (0.01 M In^{3+} or 0.01 M Zn^{2+}). Two cathodic peaks related to the reduction of each element are observed. On the one hand, the deposition of In does not occur until the cathodic potential reaches approximately −0.75 V, which is very near to the equilibrium potential of In/In^{3+}. On the other hand, the deposition of Zn occurs at a potential more positive than that obtained from solutions containing only Zn^{2+}. When the potential sweep is reversed, two well separated anodic peaks initiating close to the thermodynamic potential of Zn/Zn^{2+} and In/In^{3+} are observed. Thus, under the present conditions, the formation of alloy or intermetallic compounds between Zn and In is not expected [7, 8].

The deposition of Zn and In in sulphate solution occurs without interactions between the cathodic processes as can be deduced comparing the voltammetry obtained in the presence of both and only one of the cations (Figure 2). A potential shift of approximately

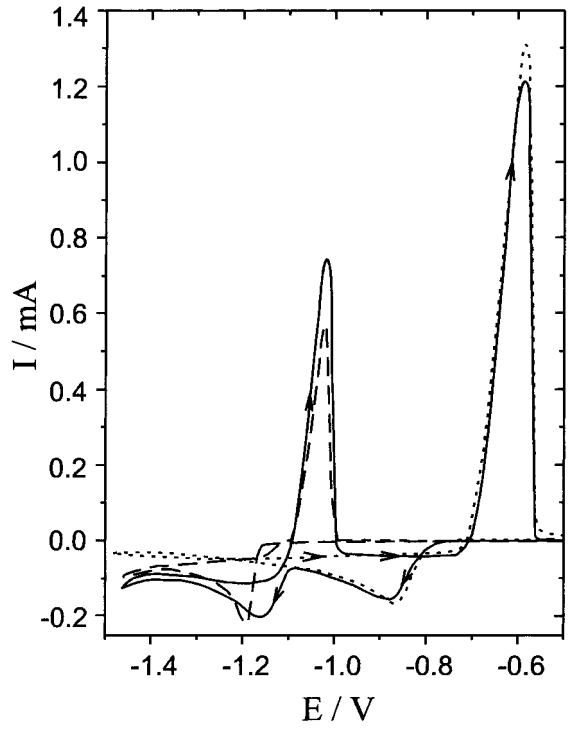

Fig. 1. Voltammetric responses of VC in 0.5 M Cl^-, pH 3 solution containing: (·····) 0.01 M In^{3+}; (----) 0.01 M Zn^{2+}; (——) 0.01 M In^{3+} + 0.01 M Zn^{2+}. $E_{s,a}$ = −0.4 V.

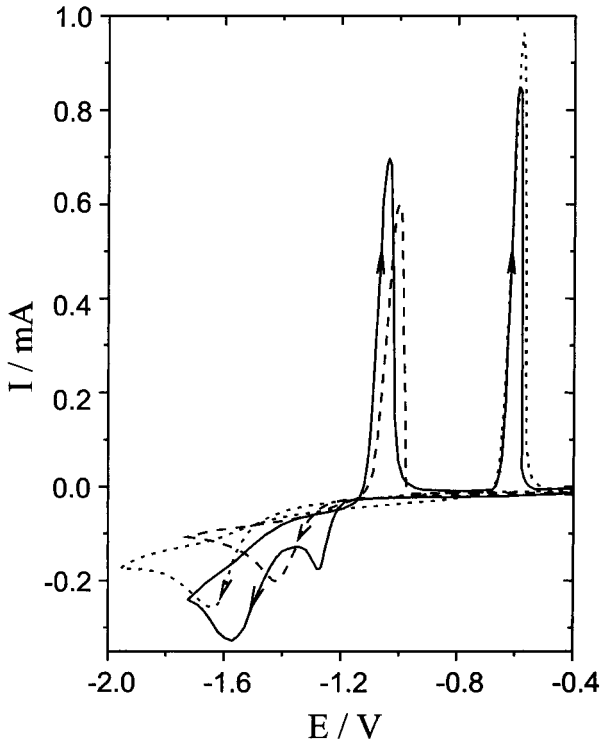

Fig. 2. Voltammetric responses of VC in 0.5 M SO_4^{2-}, pH 3 solution containing: (·····) 0.01 M In^{3+}; (----) 0.01 M Zn^{2+}; (——) 0.01 M In^{3+} + 0.01 M Zn^{2+}. $E_{s,a}$ = −0.4 V.

0.15 V towards more positive potentials is observed for In^{3+} and Zn^{2+} reduction peaks when both cations are present in solution. In this case, a high cathodic overpotential associated with massive In electrodeposition is observed. However, small In deposition currents were also detected near the thermodynamic potential of the In/In^{3+} couple [9]. In chloride solutions, the presence of Cl^- facilitates nucleation and growth of In by accelerating the rate of the reduction process [9–11].

The appearance of a potential shift for cathodic peaks observed in both chloride and sulphate solutions may be attributed to the lower energy involved in the nucleation process onto previous metallic deposits, which are already present on the VC surface.

The initial stages of nucleation of both, Zn and In, were studied using the single potentiostatic pulse method in 0.5 M Cl^- solutions. Figure 3(a) shows the I/t transients at different potential values corresponding to the deposition of Zn (dashed lines) from solution containing 0.01 M Zn^{2+}. A nondimensional analysis performed on these transients showed that nucleation follows an instantaneous regime with hemispherical diffusion controlled growth [12]. This is in agreement with results obtained by other workers [13–15].

It was shown previously that nucleation of In follows a progressive regime (Figure 3(a), solid lines) and that the actives sites of vitreous carbon may act as critical nuclei [9]. The nucleation rate shows an exponential decrease towards potentials more negative than −1.1 V. This fact was attributed to the onset of desorption of

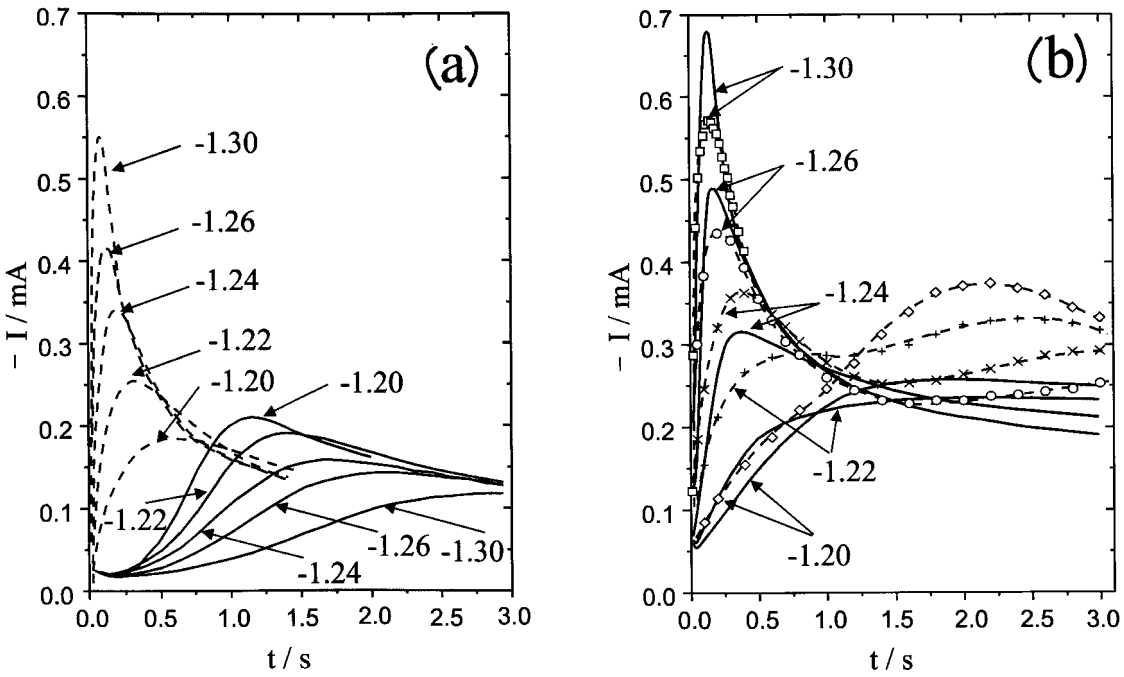

Fig. 3. Potentiostatic I/t transients registered at different potential values in 0.5 M Cl^-, pH 3 solution containing: (a) (----) 0.01 M Zn^{2+}, E_i = −0.8 V; (——) 0.01 M In^{3+}, E_i = −0.6 V; (b) (——) Experimental curves for 0.01 M Zn^{2+} + 0.01 M In^{3+}, E_i = −0.6 V; (---- and symbols) addition of curves (----) and (——) shown in (a). Potentials in V.

Cl^-, which acts as an electron bridge in the reduction process, in that potential region [9]. A similar study to that performed in [9] has shown that active sites also act as critical nuclei for the nucleation of Zn. However, in this case, an exponential growth of nucleation rate with overpotential is observed. Using the method described in [9], nucleation rate values of 7.61×10^3 s^{-1} and 1.30×10^5 s^{-1}, for the deposition of In and Zn, respectively, were calculated at a potential of −1.2 V and in the present solution conditions.

Figure 3(b) shows the I/t transients registered for increasing potential values in a 0.5 M Cl^- solution containing 0.01 M In^{3+} + 0.01 M Zn^{2+}. The transients obtained by adding the current response of the individual elements are also shown. A difference between the curves at the lower overpotentials studied is observed. This is related to the decrease in the number of active sites available for In nucleation brought about by the preferential formation of Zn nuclei. Deposition of In then occurs on the initially formed Zn deposits.

Figure 4 shows a SEM/EDX examination of the VC surface after 60 s polarization at −1.20 V. Numerous rounded grains of similar size with 55 at % of Zn on average are observed. The disappearance of the typical hexagonal shape of the deposits, which are obtained from solutions containing only Zn^{2+}, may be related to In deposition on the initially formed Zn crystallites. At higher deposition times (10 min), coalescence was achieved and deposits with 53 at % of Zn were obtained (Figure 5).

The effect of polarization time (τ) was studied by potentiodynamic anodic stripping after cathodic polarisation at −1.20 V in 0.5 M Cl^- solution (Figure 6). The voltammetric curves show only two anodic peaks, which corresponds to the oxidation of Zn and In. This result confirms that the formation of alloy or intermetallic compounds between the two metals does not occur. Nevertheless, considerable distortion of the anodic peak corresponding to Zn dissolution is observed for deposition times longer than 20 min. This is probably related to the more difficult dissolution of Zn particles embedded in the In matrix. The charge corresponding to the oxidation of each element was calculated by integration of the anodic peaks. Figure 7(a) shows the plots of Q/z (where Q is the charge and z is the oxidation number) vs cathodic polarization time for deposits obtained from solutions containing both and only one of the cations. In both cases, a linear relationship with similar slopes for each element is obtained. These results

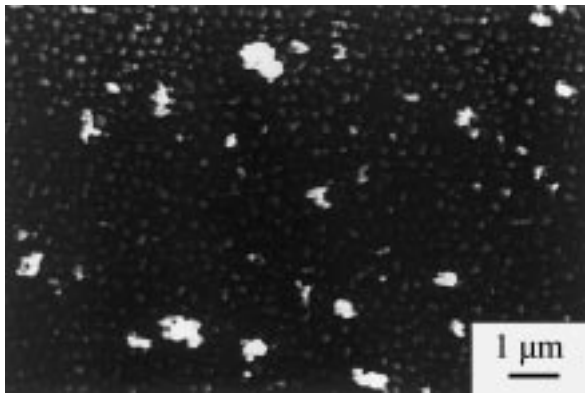

Fig. 4. SEM micrograph of the deposit obtained in 0.5 M Cl^- + 0.01 M In^{3+} + 0.01 M Zn^{2+}, pH 3 solution after 60 s at −1.2 V.

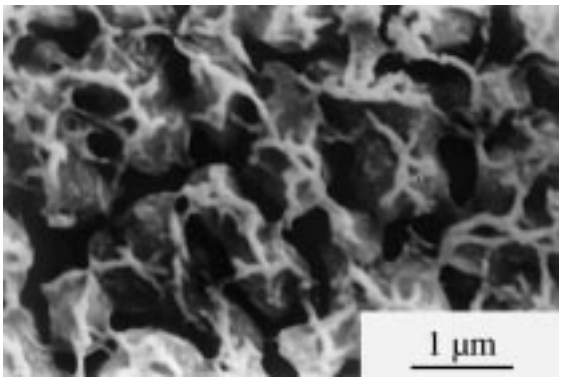

Fig. 5. SEM micrograph of the deposit obtained in 0.5 M Cl^- + 0.01 M In^{3+} + 0.01 M Zn^{2+}, pH 3 solution after 600 s at −1.2 V.

are in agreement with the constant currents shown in the I/t transients (Figure 7(b)). A higher slope value is observed when both cations are present in solution. Then, taking into account that (Q/z) is proportional to the number of atoms, the same slope for both elements is consistent with the deposit composition obtained by EDX.

Figure 8 shows the E/t profiles obtained from solutions containing only In^{3+} or Zn^{2+} after applying a constant current similar to that in the potentiostatic experiments (Figure 7(b)). Initially, the potential changes to a value close to the equilibrium potential for In/In^{3+} or Zn/Zn^{2+} couples. Then, a potential decrease, approaching values corresponding to $In/In(OH)_3$ or $Zn/Zn(OH)_2$, is observed. This suggests, that a hydroxide layer on the electrode surface is formed due to the

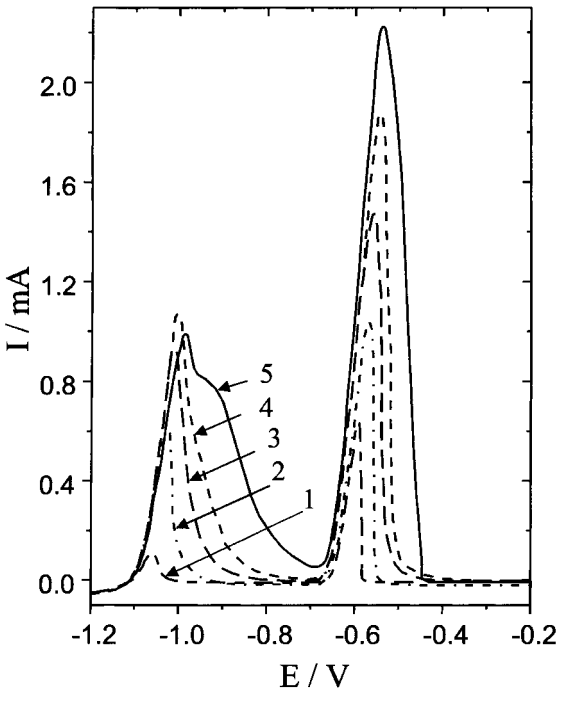

Fig. 6. Anodic stripping profiles of deposits obtained in 0.5 M Cl^- + 0.01 M In^{3+} + 0.01 M Zn^{2+}, pH 3 solution at −1.2 V after different polarization times, τ. Sweep rate: 0.005 V s^{-1}. $E_{s,c}$ = −1.2 V; $E_{s,a}$ = −0.2 V. Key: (1) 60, (2) 300, (3) 600, (4) 900 and (5) 1500 s.

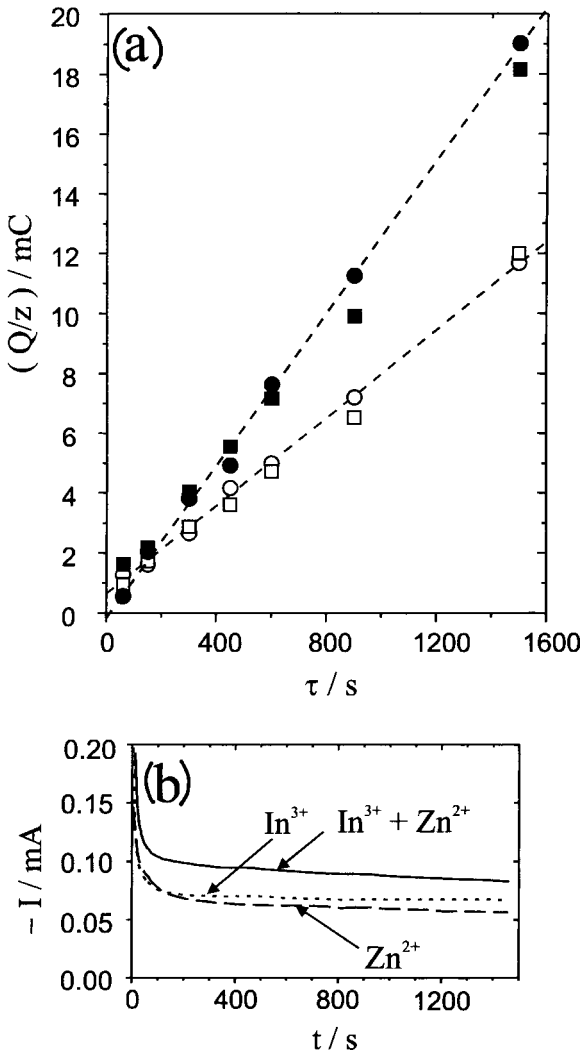

Fig. 7. (a) Anodic charge of Zn and In (as Q/z) calculated from anodic stripping of deposits obtained after different times at −1.2 V in 0.5 M Cl^-, pH 3 solution containing: (○) Zn from 0.01 M Zn^{2+}, (□) In from 0.01 M In^{3+}, (●) Zn from 0.01 M Zn^{2+} + 0.01 M In^{3+} and (■) In from 0.01 M Zn^{2+} + 0.01 M In^{3+}. (b) I/t transients at −1.2 V in: (·····) 0.01 M In^{3+}, (----) 0.01 M Zn^{2+} and (——) 0.01 M Zn^{2+} + 0.01 M In^{3+}, 0.5 M Cl^-, pH 3 solution.

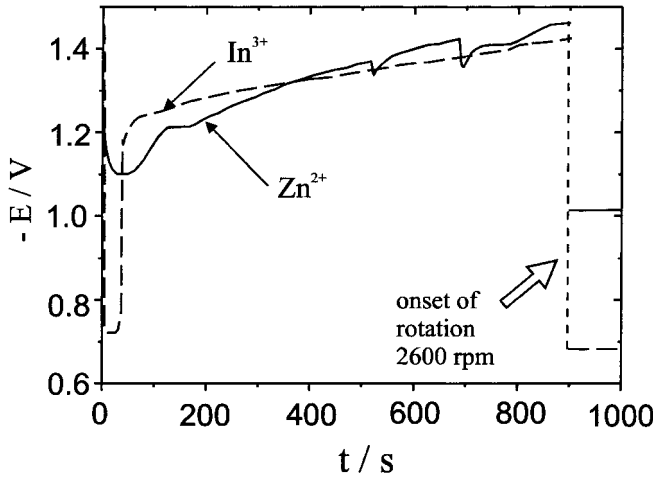

Fig. 8. Chronopotentiogram obtained during galvanostatic pulse polarization in 0.5 M Cl^-, pH 3 solution containing: (----) 0.01 M In^{3+}; (——) 0.01 M Zn^{2+}. I = 0.07 mA.

simultaneous HER. Thus, deposition may take place via the following reactions:

$$Zn(OH)_2 + 2e^- \rightarrow Zn + 2OH^- \quad (1)$$

$$In(OH)_3 + 3e^- \rightarrow In + 3OH^- \quad (2)$$

On applying electrode rotation, local alkalization is hindered and the potential shifts quickly to the In/In^{3+} or Zn/Zn^{2+} equilibrium values.

When both cations are present in solution, the pH increase at the electrode surface due to simultaneous hydrogen evolution is expected to favour the precipitation of $In(OH)_3$ rather than $Zn(OH)_2$. The effect of pH changes on the deposit composition was investigated using a 0.5 M Cl^- with acetate buffer of pH 3. The I/t response and stripping results were the same as that observed when the solution pH was adjusted to 3 by suitable addition of HCl. The presence of the buffer minimises the pH rise that takes place during electrodeposition. Precipitation of $In(OH)_3$ was detected at pH 3.42 [10], while a pH value of 7.13 was estimated for $Zn(OH)_2$ [16]. Thus, the pH increase is sufficient for the formation of In hydroxide, but not for Zn hydroxide. A similar situation was observed in the case of Zn–Co codeposition from acidic solution. However, in that case, the presence of the Zn hydroxide layer diminishes the Co deposition rate [17]. Zn and In electrodeposition occurs through an In hydroxide layer leading to deposits with the same percentage of each metal.

The higher deposition rates observed for each element from solutions containing both cations may be explained in terms of: (i) an increase in the area of metallic deposits where deposition is favoured and (ii) an increase in conductivity of the In hydroxide film due to the presence of Zn^{2+} conducting species.

3.2. *Electrodeposition of In and Zn with electrode rotation*

Figure 9 shows the effect of electrode rotation speed on the voltammetric response of vitreous carbon in 0.5 M Cl^- containing 0.01 M In^{3+} and/or 0.01 M Zn^{2+} at different pH values. For the solutions containing only In^{3+}, the cathodic current associated with In deposition approaches a limiting value. Then, a current decay is observed at more negative potentials, where adsorption of Cl^- is unlikely to occur. A similar behaviour was also observed by others on performing polarographic measurements [18]. A limiting current is also observed for the case of Zn deposition from solution containing only Zn^{2+}. At pH 2.3, a second limiting current appearing at more cathodic potentials corresponds to the hydrogen evolution.

The voltammetric curves obtained in the presence of both cations at pH 3.6, or at low rotation speed at pH 3, is similar to that obtained by adding the corresponding individual curves obtained in solutions containing only one of the cations. On the other hand, the onset of Zn

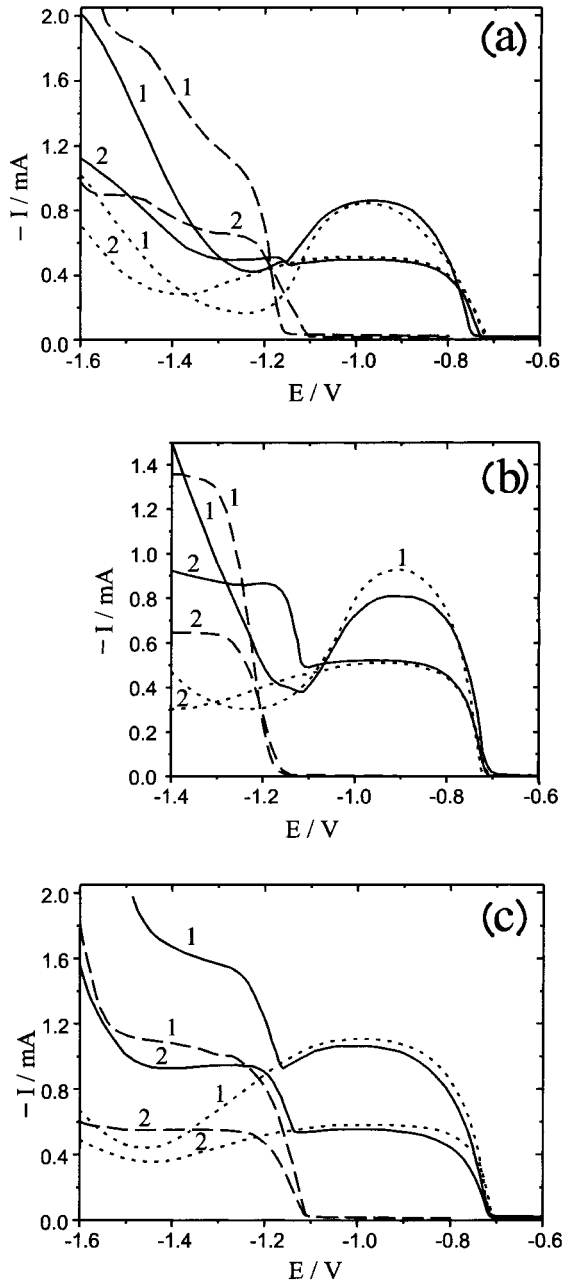

Fig. 9. Voltammetric responses registered on VC at 0.001 V s^{-1} at two electrode rotation speeds in 0.5 M Cl^- solutions of different pH and containing: (·····) 0.01 M In^{3+}; (---) 0.01 M Zn^{2+}; (——) 0.01 M Zn^{2+} + 0.01 M In^{3+}. $E_{s,c}$ = −1.6 V; $E_{s,a}$ = −0.6 V. (1) ω = 2600 rpm; (2) ω = 600 rpm. (a) pH 2.3; (b) pH 3.0; (c) pH 3.6.

deposition appears to be inhibited at pH 2.3 and the corresponding limiting current is no longer observed. The inhibiting effect can be explained in terms of a preferred adsorption of H replacing adsorbed Zn^+, this latter being an intermediate in the Zn^{2+} reduction process [19]. The approximately linear pattern of current–potential plots may be attributed to simultaneous HER.

After potentiodynamic polarization at ω = 600 rpm, a SEM/EDX analysis of a VC electrode removed at −1.40 V shows the presence of a large amount of deposit with 28 and 71 at % of Zn and In on average,

respectively (Figure 10(a)). Some hexagonal grains are observed above a compact deposit. Surprisingly, in spite of their hexagonal shape, characteristic of Zn deposits, their composition was 21 and 79 at % of Zn and In on average, respectively. A similar morphology was obtained on Al electrodes, where deposited In was found above hexagonal platelets of Zn [6]. At small ω values, it seems that deposition of In on freshly nucleated Zn is favoured.

Conversely, increased rotation speed favours the deposition of Zn. Figure 10(b) shows the deposits obtained after potentiodynamic polarization at ω = 2600 rpm. The Zn content in the deposit is now about 69 at % and increases to 77 at % for the crystallites found over the more compact deposit.

To obtain more detail on the deposition process, potentiostatic transients were obtained at −1.20 V in 0.5 M Cl^- solution containing 0.01 M In^{3+} + 0.01M Zn^{2+} at two ω values and are compared with those obtained in the presence of only one of the cations (Figure 11). The process of nucleation and growth of deposits seems to be accelerated when both cations are present in solution. This fact is probably related to a synergistic effect where nucleation of one element takes place upon the already formed metallic deposits.

Figure 12 shows the stripping profiles for deposits obtained after 60 s polarization at −1.2 V at different ω values in 0.5 M Cl^- solution containing 0.01 M In^{3+} + 0.01 M Zn^{2+}. As can be observed, the anodic peak corresponding to Zn becomes wider and is shifted towards more positive potentials upon increasing ω.

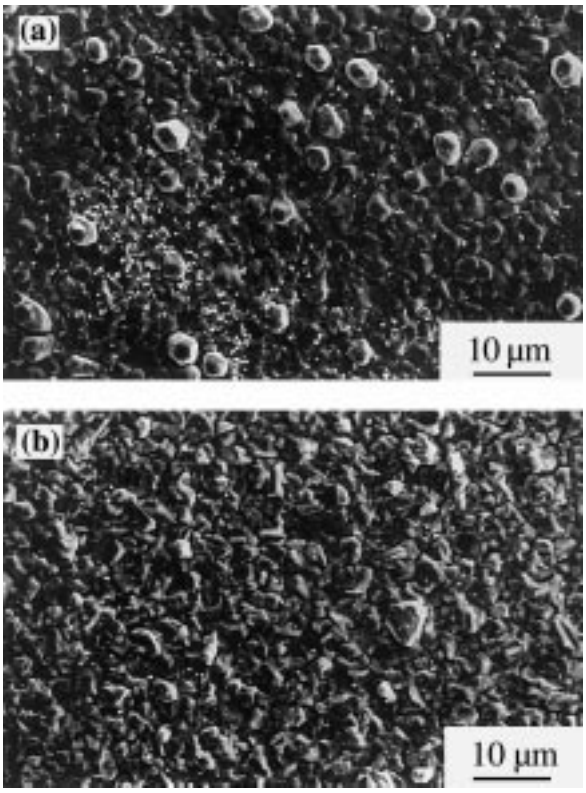

Fig. 10. SEM micrograph showing the deposit obtained by removing the VC electrode at −1.4 after potentiodynamic polarization at 0.001 V s^{-1} in 0.01 M Zn^{2+} + 0.01 M In^{3+} + 0.5 M Cl^-, pH 3 solution. (a) ω = 600 rpm; (b) ω = 2600 rpm.

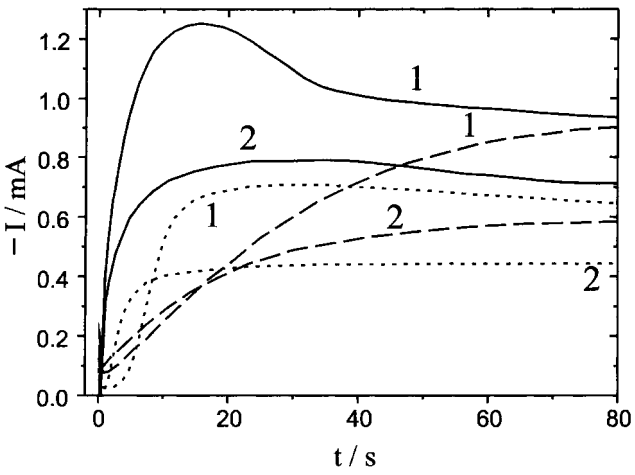

Fig. 11. Potentiostatic I/t transients obtained at −1.2 V at two electrode rotation speeds in 0.5 M Cl^-, pH 3 solution containing: (·····) 0.01 M In^{3+}; (----) 0.01 M Zn^{2+}; (——) 0.01 M In^{3+} + 0.01 M Zn^{2+}. (1) ω = 2600 rpm; (2) ω = 600 rpm. E_i = −0.4 V.

To analyse the deposit morphology after Zn dissolution, a VC electrode polarized at −1.2 V for one minute at ω = 2600 rpm was stripped in SO_4^{2-} solution and removed at −1.1 V to avoid In dissolution. The scanning electron micrograph shows a large number of holes dispersed in the deposit matrix (Figure 13), suggesting that Zn is present as segregate particles uniformly distributed. The atomic percentage of Zn in the deposit is still 13% because at −1.1 V Zn dissolution is

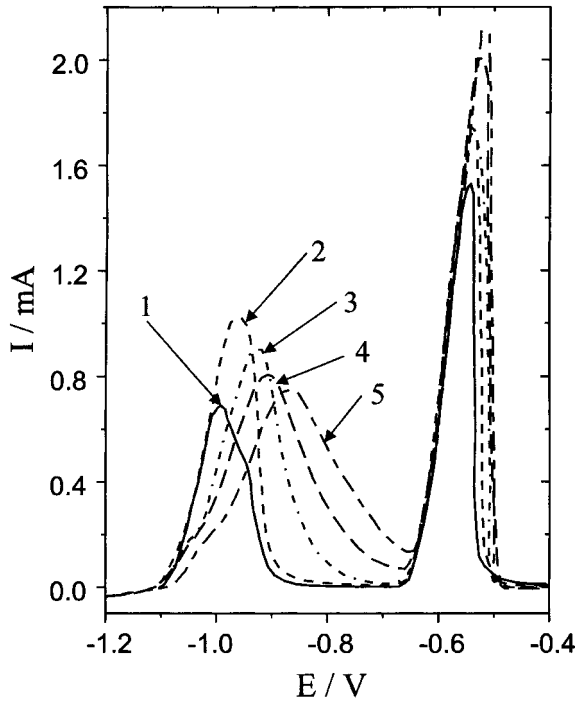

Fig. 12. Anodic stripping profiles of deposits obtained in 0.5 M Cl^- + 0.01 M In^{3+} + 0.01 M Zn^{2+}, pH 3 solution after 60 s polarization at −1.2 V under different electrode rotation speeds, ω. Sweep rate: 0.005 V s^{-1}. $E_{s,c}$ = −1.2 V; $E_{s,a}$ = −0.4 V. Key: (1) 31.41, (2) 73.30, (3) 125.66, (4) 188.49 and (5) 293.21 s^{-1}.

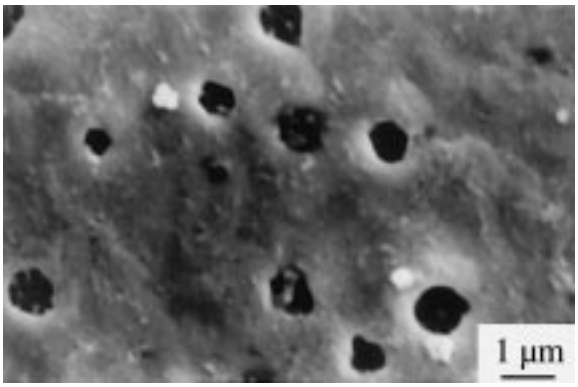

Fig. 13. SEM micrograph showing the surface after removing the electrode at −1.1 V in the anodic stripping of the deposit obtained after 60 s polarization at −1.2 V under 2600 rpm electrode rotation, in 0.5 M Cl^- + 0.01 M In^{3+} + 0.01 M Zn^{2+}, pH 3 solution.

incomplete. Therefore, the widening of the anodic peaks observed in Figure 12 may be explained in terms of a higher accumulation of Zn^{2+} inside the porous In matrix as ω increases.

Figure 14 shows the stripping charge of Zn and In, expressed as Q/z, for deposits obtained after 60 s at −1.20 V in chloride solution containing In^{3+} or Zn^{2+} at different hydrodynamic conditions (curves (a) and (b), respectively). In both cases, the amount of deposited element increases with ω but lower values are obtained for Zn dissolution. Lower current efficiencies for deposition of Zn, compared with those for In, were calculated by considering the total cathodic and the stripping charges (Figure 15). This fact can be explained taking

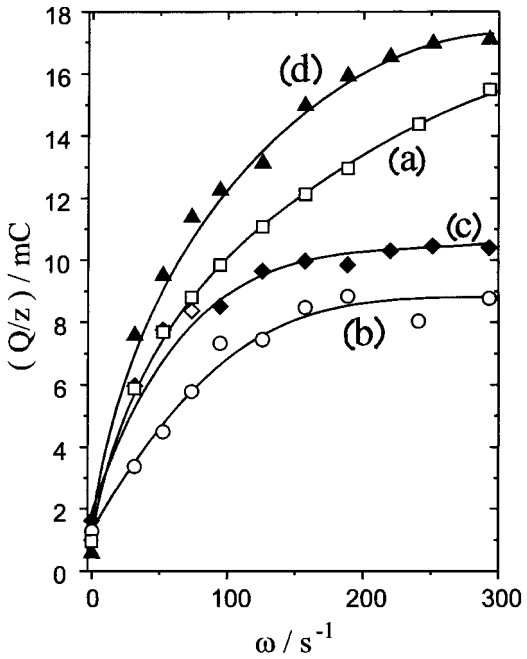

Fig. 14. Anodic charge of Zn and In (as Q/z) calculated from anodic stripping of deposits obtained after 60 s at −1.2 V with different electrode rotation speeds in 0.5 M Cl^-, pH 3 solution. (a) In from 0.01 M In^{3+}; (b) Zn from 0.01 M Zn^{2+}, (c) In from 0.01 M Zn^{2+} + 0.01 M In^{3+}; (d) Zn from 0.01 M Zn^{2+} + 0.01 M In^{3+}.

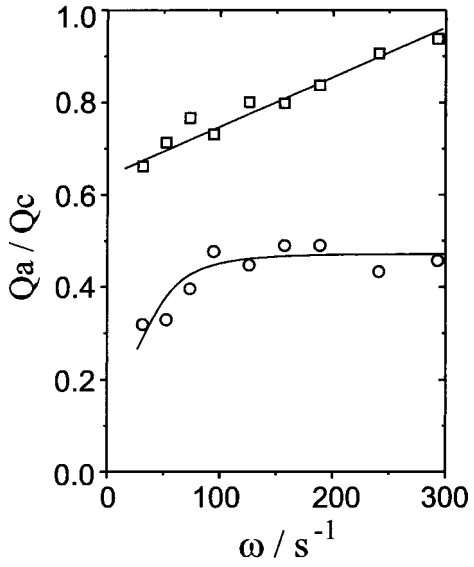

Fig. 15. Current efficiencies for deposition calculated by computing the anodic charges, obtained by stripping of deposits, and total cathodic charges after 60 s polarization at −1.2 V at different rotation speeds in 0.5 M Cl^-, pH 3 solution containing: (○) 0.01 M Zn^{2+}; (□) 0.01 M In^{3+}.

into account not only the lower overpotential for HER on Zn but also the inhibiting effect caused by preferential adsorption of H [19].

Conversely, when both cations are present in solution, the amount of deposited Zn is higher than that of In for all the rotation speeds studied (Figure 14, curves (c) and (d)). Also, the amount of In is lower than that observed when it is deposited without the presence of Zn^{2+}. Probably, the presence of In^{3+} causes a reduction in the hydrogen discharge rate by creating an additional reduction path, which leads to a higher Zn deposition rate. The species In^+, which has been postulated as an intermediate in the In^{3+} reduction process, can react with H^+ ions by [20, 22]:

$$In^+ + 2\,H^+ \rightarrow In^{3+} + H_2 \qquad (3)$$

Higher nucleation rates on In than on vitreous carbon are to be expected, if the weaker bonding energies between carbon and deposited nuclei are taken into account. Also, the overpotential for HER is higher on In than on Zn [23]. Thus, for the same potential, a lower surface coverage by adsorbed H is expected. These facts can also explain the rapid increase in current observed in the potentiostatic transients (Figure 11) and the higher Zn content for the deposits found under rotation.

4. Conclusions

The nucleation of Zn and In is favoured by the presence of previous metallic deposits. The corresponding deposition rates are also controlled by the surface pH established. Thus, under stagnant conditions, the local-

ized alkalization due to simultaneous HER, gives rise to deposition through a hydroxide layer formed on the electrode surface, leading to deposits with a similar amount of each element.

Under electrode rotation, localized alkalization is minimized and Zn rich deposits are obtained. The presence of In^{3+} can increase the Zn deposition rate in three different ways: (i) by diminishing the hydrogen evolution reaction due to reduction of H^+ by In^+ species, (ii) by formation of In deposits which favour Zn nucleation and growth on it and (iii) by the increased overpotential for HER caused by the presence of In.

Similar features were observed for the deposition of Zn and In on Al from chloride solutions under stagnant conditions. In this case, the initial deposition of Zn was favoured over In deposition. As soon as a critical amount of Zn is deposited, preferred In deposition on Zn crystallites takes place. Conversely, under electrode rotation, the discharge of Zn^{2+} is the prevalent reaction as can be observed by deposition on vitreous carbon.

Acknowledgements

Financial support from Consejo Nacional de Investigaciones Científicas y Técnicas (CONICET, PID no. 338690092) and Ciencia y Técnica UNS (UNS – CU, 0029/95) are acknowledged. Also, one of us (A.G.M.) thanks CONICET for a grant.

References

1. S. Müller, F. Holzer, J. Desilvestro and O. Haas, *J. Appl. Electrochem.* **26** (1996) 1217.
2. J.C. Lin and H.C. Shih, *J. Electrochem. Soc.* **134** (1987) 817.
3. C.B. Breslin and L.P. Friery, *Corros. Sci.* **36** (1994) 231.
4. S.B. Saidman and J.B. Bessone, *J. Appl. Electrochem.* **27** (1997) 731.
5. G. Burri, W. Luedi and O. Haas, *J. Electrochem. Soc.* **131** (1989) 2167.
6. S.B. Saidman, A.G. Muñoz and J.B. Bessone, *J. Appl. Electrochem.* **29** (1999) 245.
7. S. Swathirajan, *J. Electrochem. Soc.* **133** (1986) 671.
8. V.D. Jovic, R.M. Zejnilovic, A.R. Despic and J.S. Stevanovic, *J. Appl. Electrochem.* **18** (1988) 511.
9. A.G. Muñoz, S.B. Saidman and J.B. Bessone, *J. Electrochem. Soc.* (in press).
10. R. Piercy and N.A. Hampson, *J. Appl. Electrochem.* **5** (1975) 1.
11. V.S. Kublanovskii and S.A. Kozina, *Ukr. Khim. Zh.* **53** (1987) 500.
12. B. Scharifker and G. Hills, *Electrochim. Acta* **28** (1983) 879.
13. A.C. Beshore, B.J. Flori, G. Schade and T.J. O'Keefe, *J. Appl. Electrochem.* **17** (1987) 765.
14. A.R. Despic, and G. Pavlovic, *Electrochim. Acta* **27** (1982) 1539.
15. J. McBreen and E. Gannon, *J. Electrochem. Soc.* **10** (1983) 1667.
16. M. Pourbaix, in 'Atlas d'Equilibres Électrochimiques' (Gauthier Villars, Paris, 1963).
17. H. Yan, J. Downes, P.J. Boden and S.J. Harris, *J. Electrochem. Soc.* **143** (1996) 1577.
18. M.A. Loshkarev and A.A. Kazarov, *Elektrokhimiya* **3** (1967) 39.
19. I. Epelboin, M. Ksouri and R. Wiart, *J. Electrochem. Soc.* **122** (1975) 1206.
20. B. Miller and R.E. Visco, *J. Electrochem. Soc.* **115** (1968) 251.
21. E.E. Kobrand and L.F. Kozin, *Ukr. Khim. Zh.* **48** (1982) 1052.
22. V.V. Losev and A.P. Pchel'nikov, *Electrochim. Acta* **18** (1973) 589.
23. S. Trasatti, *J. Electroanal. Chem.* **39** (1972) 163.